Tutorial on Fault Locating Embedded in Line Current Differential Relays – Methods, Implementation, and Application Considerations

Omar Avendano
Portland General Electric

Bogdan Kasztenny, Héctor J. Altuve, Bin Le, and Normann Fischer
Schweitzer Engineering Laboratories, Inc.

Presented at the
41st Annual Western Protective Relay Conference
Spokane, Washington
October 14–16, 2014

Previously published in
Line Current Differential Protection: A Collection of Technical Papers Representing Modern Solutions, 2014

Originally presented at the
17th Annual Georgia Tech Fault and Disturbance Analysis Conference, April 2014

Tutorial on Fault Locating Embedded in Line Current Differential Relays – Methods, Implementation, and Application Considerations

Omar Avendano, *Portland General Electric*
Bogdan Kasztenny, Héctor J. Altuve, Bin Le, and Normann Fischer, *Schweitzer Engineering Laboratories, Inc.*

***Abstract*—Accurate fault locating on transmission lines becomes increasingly beneficial by allowing faster restoration of scarce power system assets back into service. Having access to synchronized remote current data, line current differential protection schemes can incorporate multiterminal fault locating algorithms, allowing for more accurate fault locating compared with single-ended methods.**

This paper describes a new fault locating algorithm for two-, three-, and four-terminal lines that is suitable for integration in a line current differential protection scheme. The paper presents the algorithm in detail, includes examples of its operation, and presents test results based on simulations as well as the testing of its actual implementation in a particular protective relay.

I. Introduction

The increasing availability of reliable digital communications in electric utilities promotes applications of line current differential (87L) schemes. Responding to all currents of the protection zone, the current differential principle is sensitive, inherently selective, and secure. Also, differential protection is typically easy to apply because it does not require detailed short-circuit studies and settings calculations. In its application to power lines, the principle is minimally or not affected by weak terminals, series compensation, changing short-circuit levels, power swings, nonstandard short-circuit current sources, and many other issues relevant for protection techniques based on measurements from a single line end [1].

Accurate fault locating on transmission lines becomes more important as margins in present power systems erode, requiring fast restoration of transmission lines after faults.

Embedding multiterminal fault locating algorithms in 87L relays is a natural fit. First, fault locators embedded in 87L schemes benefit from the data time alignment already in place for the 87L protection elements and, as such, can often be applied without external time sources for synchronization, such as Global Positioning System (GPS) clocks.

Second, the embedded fault locators use the existing 87L communications channels, avoiding extra investment and complexity compared with standalone multiterminal fault locators.

The following factors make the fault locators embedded in 87L relays belong to a separate category of fault locating methods:

- As a rule, the 87L scheme has access to remote currents, but not necessarily to remote voltages. As a result, many implementations use local voltages and currents but only remote currents.
- The scheme may have permanently or temporarily reduced accuracy of data synchronization. Reduced accuracy may be acceptable for protection functions, but can be very detrimental for fault locating and therefore requires special attention.
- The scheme may lose communications between some relays and operate in a master-slave mode, with only one relay having access to remote data. When some or all communications are lost, the fault locator may need to fall back into a single-ended backup mode. This requires the fault locator to be adaptive, depending on the availability of remote data.
- 87L relays can be applied to multiterminal lines. Their embedded fault locators determine the faulted segment of the line in addition to the distance to the fault.
- 87L schemes must remain fully operational after the fault is cleared and during reclosing. Therefore, any additional usage of the channel for fault locating purposes must be carefully engineered so as not to negatively impact the line protection.
- Line charging currents on long lines and cables will affect the fault locating accuracy. Some 87L relays compensate for the charging current. Their embedded fault locators can take advantage of this compensation to increase their accuracy.

This paper presents a new fault locating algorithm that is optimized specifically for implementation in a typical 87L scheme and that addresses the following design criteria and requirements:

- Minimize the channel bandwidth requirements of the fault locator without increasing the amount of data sent in real time over the existing 87L channel.

- Identify the faulted line section in three- and four-terminal applications without the need to exchange voltage measurements between the 87L relays.
- Report consistent fault location in all relays of the 87L scheme.
- Reduce the impact of fault resistance and its variability on the fault locating accuracy.
- Detect the loss of precise data synchronization in the scheme and fall back accordingly so that the fault locating accuracy is not adversely impacted by misalignment between the local and remote currents.
- Support the master-slave mode of 87L scheme operation.
- Continue providing fault location information based on a single-ended algorithm upon a total loss of data synchronization or communications.

In Section II, we review the fundamentals of fault locating for two-terminal and three-terminal lines. In Section III, we introduce a new fault locating algorithm, illustrate its operation with an example, and discuss its accuracy. In Section IV, we explain how the new algorithm is applied to perform fault locating in three-terminal lines and how the scheme functions in a master-slave configuration. In Section V, we discuss how the algorithm is implemented for a four-terminal line. Finally, we provide some key conclusions.

II. Review of Multi-Ended Fault Locating Methods

Various fault locating methods have been introduced over the last several decades. These methods are based on traveling waves [2] or impedance measurements [3], which each include single-ended [4] and double-ended [5] methods. This paper covers impedance-based fault locating methods only.

As the number of transmission lines with more than two terminals has increased over the last few years, so has the need for more accurate fault locating on these multiterminal lines. This paper shows that one type of double-ended fault locating method can be adapted for locating faults on multiterminal lines.

We begin by reviewing the two-ended fault locating methods. The problem to solve is to determine the distance to the fault (*m*) from the selected line terminal, as shown in Fig. 1.

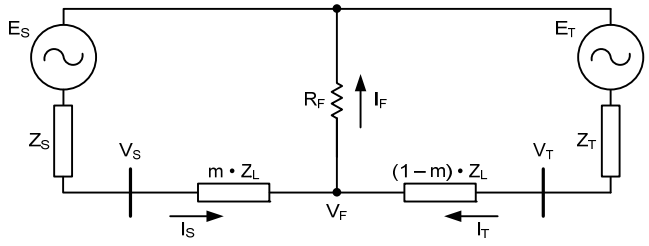

Fig. 1. Equivalent diagram of a two-terminal line with a fault at *m* per unit (pu) from Terminal S, with fault resistance R_F.

The method used to determine fault location on a two-terminal line depends on the data available. The types of data available are as follows:

- Local voltage and current only (single-ended method).
- Local voltage and current plus time-aligned remote current.
- Time-aligned local and remote voltages and currents.
- Local and remote voltages and currents that are not time-aligned.

In this paper, we concentrate on double-ended fault locating methods. When double-ended methods are employed, fault locating can be done in real time or offline. Typically, data generated by a line distance relay or any device that does not have access to remote data will be processed offline. Data measured by an 87L relay will typically be processed in real time.

A. Two-Ended Method With Synchronized Voltage and Current Measurements

When data are available from both line terminals, we apply Kirchhoff's voltage law to the voltage and current phasors in the Fig. 1 circuit.

$$\begin{aligned} V_F &= V_S - m \bullet Z_L \bullet I_S \\ V_F &= V_T - (1-m) \bullet Z_L \bullet I_T \end{aligned} \tag{1}$$

If the measurements at both line terminals are time-aligned (synchronized), then we can solve for *m* as follows:

$$m = \frac{(V_S - V_T) + Z_L \bullet I_T}{Z_L \bullet (I_S + I_T)} \tag{2}$$

Equation (2) can be applied to any of the symmetrical component networks to solve for *m*.

B. Two-Ended Method With Nonsynchronized Voltage and Current Measurements

If the measurements at the line terminals are not time-aligned (nonsynchronized), then it is convenient to use the negative-sequence network to solve for *m* for unbalanced faults. Because the negative-sequence network is not influenced by balanced load, load current will not affect the fault location calculation. In addition, the negative-sequence network is almost unaffected by charging current and is less susceptible to mutual coupling effects than the zero-sequence network [5]. Furthermore, negative-sequence quantities are available for all unbalanced faults, while zero-sequence quantities are available only for ground faults.

Fig. 2 is the negative-sequence network for the fault condition shown in Fig. 1, valid for any unbalanced fault.

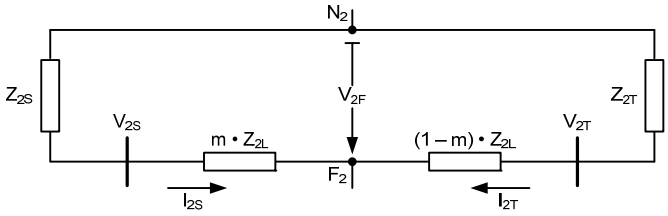

Fig. 2. Negative-sequence network for the fault condition shown in Fig. 1.

The magnitudes of the fault voltages calculated in (1) using the local and remote voltages and currents match even though the local and remote measurements are not synchronized. Therefore, we can write (3).

$$\left|V_{2S} - m \bullet Z_{2L} \bullet I_{2S}\right| = \left|V_{2T} - (1-m) \bullet Z_{2L} \bullet I_{2T}\right| \qquad (3)$$

If we square the terms on the left-hand side and right-hand side of (3) and rearrange terms, we obtain the following quadratic equation:

$$Xm^2 + Ym + Z = 0 \qquad (4)$$

where:

X, Y, and Z are functions of Z_{2L}, V_{2S}, V_{2T}, I_{2S}, and I_{2T}.

Solving (4), we obtain two values for *m*, a value less than zero and a value greater than zero. The value of *m* greater than zero is the solution for the distance to the fault. References [1] and [5] describe this method in detail.

C. Two-Ended Method for Nonhomogeneous Transmission Lines

There are nonhomogeneous transmission lines where part of the line is an overhead line and part is a cable. For this type of line configuration, we cannot simply apply the two-ended fault locating methods described previously and expect accurate results. One applicable method uses synchronized voltages and currents from both line terminals and solves the negative-sequence network for the fault location.

Assume that a nonhomogeneous line composed of an overhead section and an underground section experiences an unbalanced fault at a distance *m* from Terminal S, as shown in Fig. 3.

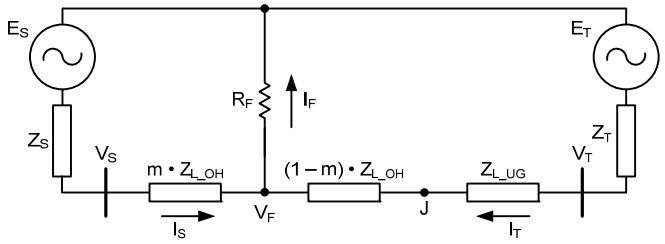

Fig. 3. Equivalent diagram of a nonhomogeneous two-terminal line with a fault at *m* pu from Terminal S. J is the junction point of the overhead and underground sections.

Fig. 4 is the negative-sequence network for the fault condition shown in Fig. 3.

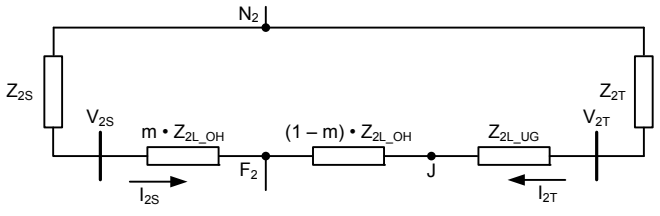

Fig. 4. Negative-sequence network of a nonhomogeneous two-terminal line with a fault at *m* pu from Terminal S.

Using the sequence network in Fig. 4 and the negative-sequence voltages and currents from the respective terminals, we can calculate the negative-sequence voltage at Junction Point J and the remote terminal (T or S) twice, starting from each line terminal, in order to construct two negative-sequence voltage profiles [6]. From Fig. 4, we derive (5), the two negative-sequence voltages calculated at Terminal S.

$$\begin{aligned} V_{2\_SJ} &= V_{2S} - Z_{2L\_OH} \bullet I_{2S} \\ V_{2\_ST} &= V_{2S} - \left(Z_{2L\_OH} + Z_{2L\_UG}\right) \bullet I_{2S} \end{aligned} \qquad (5)$$

Similarly, we derive (6), the two negative-sequence voltages calculated at Terminal T.

$$\begin{aligned} V_{2\_TJ} &= V_{2T} - Z_{2L\_UG} \bullet I_{2T} \\ V_{2\_TS} &= V_{2T} - \left(Z_{2L\_OH} + Z_{2L\_UG}\right) \bullet I_{2T} \end{aligned} \qquad (6)$$

Plotting the magnitudes of the negative-sequence voltages given by (5) and (6), we obtain the negative-sequence voltage magnitude profiles depicted in Fig. 5. As shown in this figure, the location at which the two voltage magnitude profiles intersect is the fault location we seek.

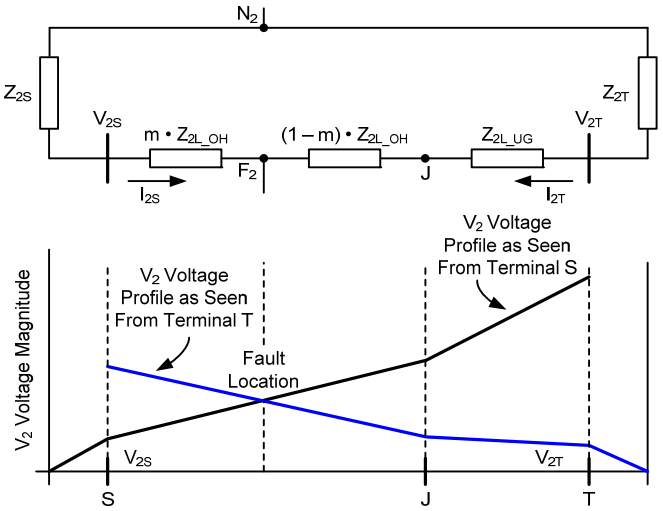

Fig. 5. Negative-sequence voltage magnitude profiles as seen from both line terminals. The intersection of the profiles indicates the fault location.

D. Three-Ended Method

One method of calculating the fault location on a three-terminal line is to convert the three-terminal line to an equivalent two-terminal line and apply one of the methods discussed previously to determine the fault location [6].

1) Synchronized Line Terminal Measurements

When the measurements at all three terminals are synchronized, it is easy to obtain the two-terminal equivalent of the three-terminal line. Assume a fault occurs at a distance *m* from Terminal S of a three-terminal line, as shown in Fig. 6.

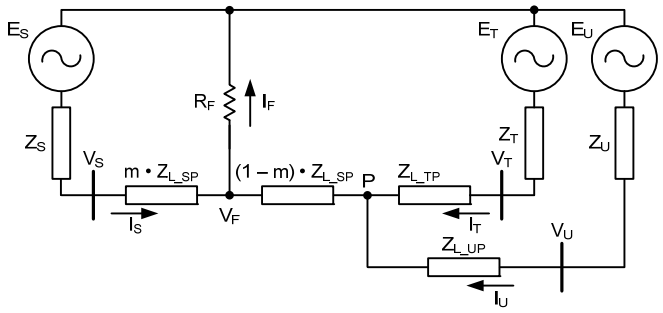

Fig. 6. Fault on a three-terminal line at *m* pu from Terminal S.

The first step to obtain the two-terminal equivalent of the three-terminal line is to calculate the voltage at Tap Point P from each line terminal. We can use either the positive-sequence network (for three-phase faults) or the negative-sequence network (for unbalanced faults). For example, Fig. 7 shows the negative-sequence network for the case of an unbalanced fault in the Fig. 6 system.

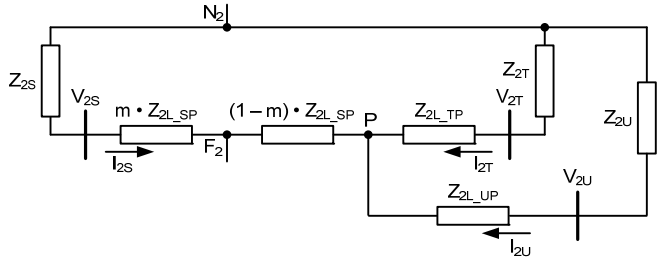

Fig. 7. Negative-sequence network for an unbalanced fault at *m* pu from Terminal S in the Fig. 6 system.

Using the negative-sequence voltages and currents measured at the line terminals and the impedances of the line sections, we calculate the negative-sequence voltages at the tap point using (7).

$$\begin{aligned} V_{2\_SP} &= V_{2S} - Z_{2L\_SP} \bullet I_{2S} \\ V_{2\_TP} &= V_{2T} - Z_{2L\_TP} \bullet I_{2T} \\ V_{2\_UP} &= V_{2U} - Z_{2L\_UP} \bullet I_{2U} \end{aligned} \tag{7}$$

The negative-sequence tap-point voltages calculated for the two unfaulted line sections will match (for our case, $V_{2\_TP} = V_{2\_UP}$). The negative-sequence tap-point voltage magnitude calculated from the faulted line section terminal will typically be much higher than the tap-point voltage calculated from the unfaulted line section terminals. This allows us to identify the faulted section of the line. If all three tap-point voltages are equal, then the fault is at the tap point.

Because current measurements are synchronized, we can combine the two unfaulted line sections into one equivalent terminal by adding their currents together and using the tap-point voltage as the equivalent terminal voltage. Fig. 8 shows the resulting negative-sequence two-terminal equivalent of the faulted three-terminal line.

Once we have the two-terminal equivalent of the three-terminal line for the case with synchronized measurements, we can apply the method described in Section II, Subsection A and use (2) to determine the fault location.

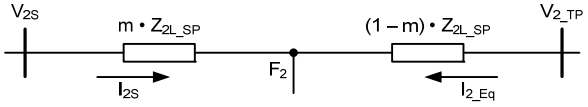

Fig. 8. Negative-sequence two-terminal equivalent of the faulted three-terminal line of the Fig. 7 network for the case when measurements are synchronized.

2) Nonsynchronized Line Terminal Measurements

When the measurements are not synchronized, the approach to obtain the two-terminal equivalent of the three-terminal line is similar to the case with synchronized measurements. We first calculate the negative-sequence tap-point voltage using (7). The magnitudes of the tap-point voltages calculated for the unfaulted line sections will be the same, but their angles will be different because of the lack of measurement synchronization. Adding the two negative-sequence currents to form an equivalent terminal current is not possible in this case. However, we can calculate the correction angle needed to align the currents by using the tap-point voltages calculated for the two unfaulted line sections, as shown in (8).

$$\text{Align} = \angle V_{2\_TP} - \angle V_{2\_UP} \tag{8}$$

Knowing the alignment angle, we can now calculate the equivalent terminal current using (9).

$$I_{2\_Eq} = I_{2T} + I_{2U} \bullet 1\angle\text{Align} \tag{9}$$

Using V_{2_TP} and I_{2_Eq} as the negative-sequence voltage and current of the equivalent terminal, we can create the negative-sequence two-terminal equivalent of the faulted three-terminal line shown in Fig. 9.

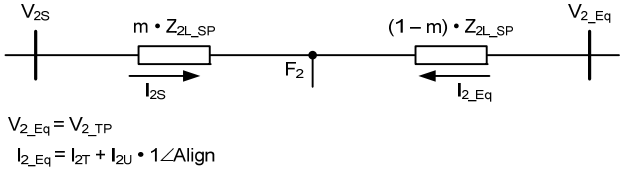

Fig. 9. Negative-sequence two-terminal equivalent of the faulted three-terminal line of the Fig. 7 network for the case when measurements are not synchronized.

Once we have the two-terminal equivalent of the three-terminal line for the case with nonsynchronized measurements, we can apply the method described in Section II, Subsection B and use (4) to determine the fault location.

III. Two-Ended Fault Locating in 87L Relays

This section introduces a two-ended fault locating algorithm as implemented in an 87L relay. This algorithm is directly applicable to two-terminal lines and is also a part of the fault locating scheme in three- and four-terminal line applications.

A. Fundamentals

When looking at the faulted line from a single line terminal and trying to find the fault location, we deal with one more unknown than the number of equations available.

Single-ended methods solve this problem by making reasonable assumptions or approximations. Different assumptions yield different fault locating methods. Two-ended methods solve this problem by obtaining at least one measurement from the other end of the line.

Consider the two-terminal line shown in Fig. 1 with a fault at *m* pu from Terminal S. The distance to the fault from Terminal S can be calculated using the following fundamental equation [1]:

$$m = \frac{\mathrm{Im}\left(V_S \bullet I_F^*\right)}{\mathrm{Im}\left(I_S \bullet Z_L \bullet I_F^*\right)} \tag{10}$$

where:

* is the complex conjugate operator.

Neglecting measurement errors in the current (I_S) and voltage (V_S) phasors, errors in the line impedance (Z_L) value (magnitude and angle), system nonhomogeneity, and the impact of charging current, (10) yields accurate results regardless of prefault power flow and fault resistance.

The obvious challenge in implementing (10) is that the fault current I_F is unknown to any single-ended method. By the nature of (10), however, only the angle of the fault current is required. This angle can be reasonably approximated with the angle of the local incremental current (Takagi algorithm) or with the local negative-sequence current or zero-sequence current (whichever sequence network is more homogeneous). This solution leads to a practical and, for most operating conditions, accurate single-ended algorithm (Schweitzer method [4] [7]).

Fig. 10 illustrates this particular approach for a single-line-to-ground fault.

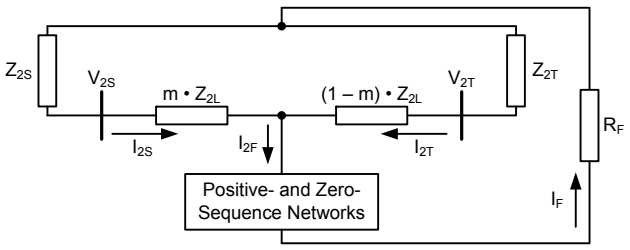

Fig. 10. Negative-sequence voltage and current quantities for a single-line-to-ground fault.

From Fig. 10, it is clear that:

$$\angle I_F \approx \angle I_{2S} \approx \angle I_{2T} \tag{11}$$

Similarly, from the zero-sequence network (not shown in Fig. 10), we can write (12).

$$\angle I_F \approx \angle I_{0S} \approx \angle I_{0T} \tag{12}$$

Equations (11) and (12) are true as long as the negative- and zero-sequence networks are homogeneous (i.e., the angles of the total system impedances at the left and right sides of the fault point in Fig. 10 are similar).

Practical implementations of this method require fault type identification and use of the proper loop quantities in order to reflect the positive-sequence impedance between the line terminal and the fault point. For example, for AG faults, we apply (13).

$$m = \frac{\mathrm{Im}\left(V_{AS} \bullet I_{2S}^*\right)}{\mathrm{Im}\left(\left(I_{AS} + k_0 \bullet I_{0S}\right) \bullet Z_{1L} \bullet I_{2S}^*\right)} \tag{13}$$

where:

k_0 is the zero-sequence current compensating factor.

The use of local negative-sequence current in (13) is referred to as polarization. The method of (13) is widely used and performs well as long as the negative-sequence network is homogeneous (which is typically the case) [1] [7].

This method is further enhanced to create a new method (described in the next subsection) and becomes a fallback method in our 87L implementation should the loss of communications or loss of data alignment prevent use of the new method.

B. Effect of Polarizing Quantities on Fault Locating

Fig. 10 shows that the fault current (normally not available to any single-ended protection scheme) is the differential current I_{DIF} naturally available to the 87L scheme.

$$I_F = I_S + I_T = I_{DIF} \tag{14}$$

As a result, (10) is not theoretical anymore but can be practically implemented by substituting the fault current with the 87L differential current I_{DIF}. For example, for AG faults as seen from Terminal S, we apply (15).

$$m = \frac{\mathrm{Im}\left(V_{AS} \bullet I_{2DIF}^*\right)}{\mathrm{Im}\left(\left(I_{AS} + k_0 \bullet I_{0S}\right) \bullet Z_{1L} \bullet I_{2DIF}^*\right)} \tag{15}$$

We used the two-machine sample system shown in Fig. 11 to illustrate the performance of the new fault locating algorithm shown in (15). The parallel lines in the figure are mutually coupled. Fig. 11 also shows the impedance values measured by a distance element for faults at different locations (different *m* values from Terminal S) that were calculated in subsequent simulations and are represented by dots in the figure. We simulated high fault resistance values and a strong infeed effect, which caused the apparent impedance to shift considerably to the right from the line impedance in the figure.

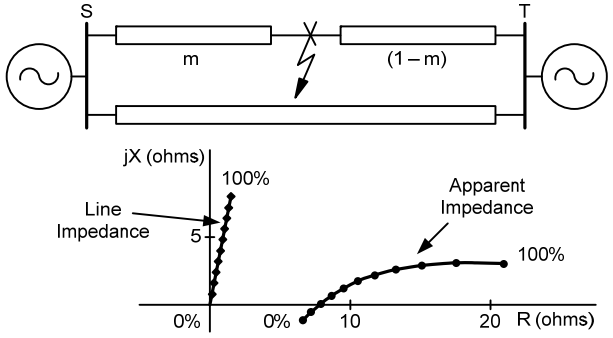

Fig. 11. Impedances measured by a distance element for faults at different locations on a two-terminal line mutually coupled with an adjacent parallel line.

Fig. 12 plots the fault locating results for the fault cases shown in Fig. 11. The figure depicts the calculated *m* values (from Terminal S) when using the Terminal S negative-sequence current, Terminal S zero-sequence current, and differential negative-sequence current for polarization.

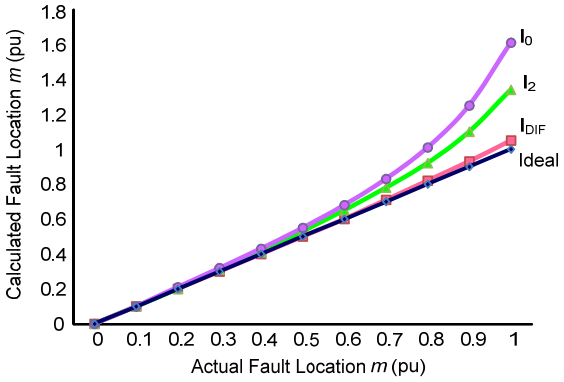

Fig. 12. Comparison of fault locating results for the Fig. 11 fault cases using Terminal S zero- and negative-sequence currents and the differential negative-sequence current for polarization.

Polarizing with the differential current (new method) gives the best results. The accuracy is only slightly degraded for faults close to the remote line terminal because of the impact of the zero-sequence mutual coupling with the parallel line. (The fault locating algorithm has no mutual coupling compensation in this example.)

Using the local negative-sequence current gives good results for close-in faults. However, when the fault is farther away from the terminal, the results are less accurate. This error is caused by network nonhomogeneity. In this example, the angle of the remote source negative-sequence impedance is different from the angle of the equivalent negative-sequence impedance of the line and local source. As the fault moves away from Terminal S, the negative-sequence network seen from the fault point becomes less homogeneous. Using the local zero-sequence current gives even worse results because we modeled higher nonhomogeneity in the zero-sequence network (which is a typical situation) and because the zero-sequence network is more affected by mutual coupling than the negative-sequence network is.

Of course, for low fault resistance values or with light load on the line, these three polarizing methods would yield good fault locating accuracy [7]. In practical situations, however, the new method using the differential current for polarization gives much better results.

C. Factors That Affect Fault Locating Accuracy

The accuracy of the described fault locating method can be analyzed based on (15). In particular:

- The algorithm uses line positive- and zero-sequence impedances and is affected by errors in their values. In particular, the zero-sequence impedance (buried in the k_0 factor) is typically known with less accuracy and may change seasonally because of soil resistivity and conductor sag due to heat or ice.
- The algorithm is impedance-based and therefore affected by line asymmetry. Even fully transposed lines are symmetrical only between their terminals. The two line segments created by a randomly located fault are not symmetrical, in general.
- The algorithm is affected by mutual coupling for ground faults.
- Errors in measuring the currents and voltages affect the accuracy, as in any impedance-based algorithm.
- Last, but not least, phase errors in the polarizing signal (the differential current) impact the fault locating accuracy. This source of error is unique to the new method and is explained next.

87L relays need to time-align the remote and local currents before forming the differential current. Two methods are used in practice for current alignment. When the channel is symmetrical (equal latencies in the transmitting and receiving directions), 87L schemes typically align the data using the industry standard method known as the ping-pong algorithm [8]. When the channel is not symmetrical, the ping-pong algorithm introduces a time-alignment error proportional to the amount of asymmetry. The resulting current phase error creates a fictitious phase shift in the differential current during internal faults.

When using asymmetrical channels, 87L relays require a common (external) time reference to align the currents [8]. Historically, GPS clocks have been used as the time reference. These clocks may be embedded in the 87L relays (rare) or be standalone and connected via an IRIG-B input (more common). More recently, terrestrial network-based time-distribution systems have also been used.

In any case, a small phase angle error in the differential current (perfectly tolerable by the 87L protection elements) would cause a considerable fault locating error using (15). To illustrate this error, consider the system in Fig. 11 and assume a phase error in the range of ±10 degrees in the differential current. Fig. 13 shows the fault locating results using the differential current for polarization.

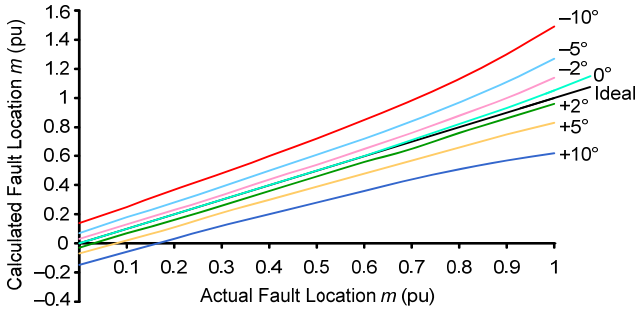

Fig. 13. Effect of phase errors in the differential current on the fault locating accuracy using (15) in the sample system in Fig. 11.

Consider, for example, an error of 5 degrees. Assuming a perfectly homogeneous network, the local and remote negative-sequence currents are perfectly in phase for an internal fault. If their magnitudes are equal, it would take a shift in the remote current of 10 degrees in order to shift the differential current by 5 degrees. A 10-degree shift in a 60 Hz

system can be caused by channel asymmetry equal to 2 • (10 degrees/360 degrees)/60 Hz = 0.93 milliseconds.

This level of asymmetry is well within the tolerance of a typical 87L protection scheme, but in the system of Fig. 11, it would cause a fault locating error in the order of 10 to 20 percent, as shown in Fig. 13.

Therefore, the precision of current data alignment must be monitored by the fault locator embedded in the 87L scheme. The basic principle of monitoring the precision of data alignment works as follows:

- When in the time-based mode (GPS), each relay of the 87L scheme must be locked to a precise time source. If the lock is lost or the source of time (clock) reports a time error via the IEEE C37.118-compliant time quality bits in the IRIG-B signal, the precision of current data alignment is declared low for use in the embedded fault locator.
- When in the channel-based mode (ping-pong), if the angle difference between the local negative-sequence current and the differential negative-sequence current is greater than a threshold (a few degrees), the precision of data alignment is declared low.

Upon detected or suspected poor precision of current data alignment, the algorithm falls back from the version given by (15) to the single-ended version given by (13).

D. Results Obtained From Field Events

We used two actual fault cases, courtesy of Bonneville Power Administration (BPA), to evaluate the single- and double-ended fault locating algorithms. Both faults occurred on the BPA Goshen-Drummond line. This line has a length of 117.11 kilometers and is effectively symmetrical because it has a large number of different tower configurations. This line shares towers with another line for a portion of its run. Therefore, mutual coupling is a factor for single-line-to-ground faults.

Table I gives the fault type, the actual fault distance determined by the field crew, the fault distance estimated by the single-ended fault locating algorithm and its error, and the fault distance estimated by the double-ended fault locating algorithm and its error. Fault distances are given from the Goshen terminal end. The percentage error was calculated as defined by IEEE C37.114 [9].

$$\%\ \text{Error} = \frac{\left|\text{Actual Distance} - \text{Calculated Distance}\right|}{\text{Line Length}} \bullet 100 \quad (16)$$

TABLE I
PERFORMANCE OF THE SINGLE- AND DOUBLE-ENDED FAULT LOCATING ALGORITHMS FOR TWO ACTUAL FAULTS

Fault Type	Actual Distance (km)	Single-Ended Method		Double-Ended Method	
		Distance (km)	Error (%)	Distance (km)	Error (%)
CG	109.29	105.42	3.30	106.24	2.60
BG	61.41	54.77	5.67	60.69	0.61

Table I shows that the double-ended fault locating algorithm is more accurate than the single-ended algorithm for both faults. However, for the CG fault, the accuracies of both methods are about the same. The reason for the similar accuracies is that the CG fault resistance was very low, which makes both methods behave similarly. The other causes of fault locating errors discussed in the previous subsection affect the single- and double-ended methods similarly. In this particular case, even though the line is symmetrical when observed from the line terminals, it is not symmetrical when viewed from the fault point. Therefore, the error is caused by the asymmetry of the transmission line when viewed from the fault location. In addition, mutual coupling affects both fault locating methods.

In the BG fault, the fault resistance had a higher value. The accuracy advantage of the double-ended algorithm over the single-ended algorithm is more evident in this case.

IV. THREE-ENDED FAULT LOCATING IN 87L RELAYS

For multiterminal lines, the fault locating process is performed in two steps. First, each relay calculates the fault location and sends the result to the other relays. Second, each relay uses the fault location information from all of the terminals to determine the faulted line section and the distance to the fault.

A. Faulted Section Identification and Fault Location Determination

The method presented in Section III, Subsection B requires the 87L relays to exchange their individually calculated fault location values (*m* values) in per unit with each other when applied to three- and four-terminal lines. This exchange is accomplished using a patent-pending method of provisioning two bits in an 87L data packet and modulating these bits to facilitate a virtual serial communication over the 87L channel.

Consider the three-terminal line shown in Fig. 14. Three 87L relays comprise the 87L scheme. Each relay has access to the local voltages and currents as well as to the remote currents (the method described in this paper does not need access to the remote voltages).

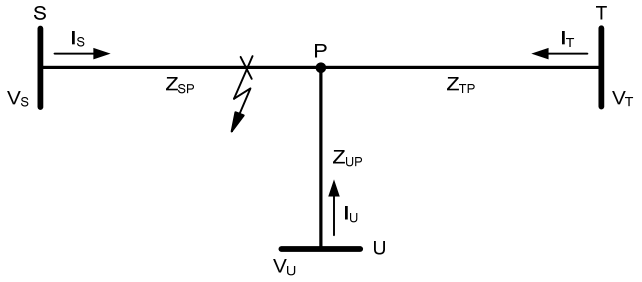

Fig. 14. Three-terminal line.

For the method described in this paper, each relay assumes the fault to be in its local section of the line and uses (15) to calculate the fault location.

The relay at Terminal S calculates:

$$m_S = \frac{\mathrm{Im}\left(V_S \bullet I_{DIF}^{*}\right)}{\mathrm{Im}\left(I_S \bullet Z_{SP} \bullet I_{DIF}^{*}\right)} \quad (17a)$$

The relay at Terminal T calculates:

$$m_T = \frac{\mathrm{Im}\left(V_T \bullet I_{DIF}^{*}\right)}{\mathrm{Im}\left(I_T \bullet Z_{TP} \bullet I_{DIF}^{*}\right)} \quad (17b)$$

The relay at Terminal U calculates:

$$m_U = \frac{\mathrm{Im}\left(V_U \bullet I_{DIF}^{*}\right)}{\mathrm{Im}\left(I_U \bullet Z_{UP} \bullet I_{DIF}^{*}\right)} \quad (17c)$$

If the fault is actually on Section SP of the line (as shown in Fig. 14), $m_S < 1$ pu. If the fault is beyond Tap Point P, $m_S > 1$ pu. The method is very unlikely to overreach (i.e., indicate $m_S < 1$ pu for a fault beyond the tap point).

For a fault beyond the tap point, extra current flows toward the fault on the faulted section (infeed effect), elevating the voltage at the relay location. The relay measures the increased voltage but not the additional current. Consider the 87L relay at Terminal T in Fig. 14. Current I_U produces a voltage drop between the tap point and the fault, but this current is not measured by the relay at Terminal T. As a result, m_T will very likely be greater than 1 pu, regardless of the power flow through the line.

For example, under one power flow pattern in the system of Fig. 14 (power flow from Terminal T to Terminals S and U), the following results were obtained for a fault at $m = 0.9$ pu from Terminal S: $m_S = 0.91$ pu, $m_T = 1.30$ pu, and $m_U = 1.55$ pu. Under a different power flow pattern (power flow from Terminals S and U to Terminal T), the following results were obtained: $m_S = 0.89$ pu, $m_T = 1.57$ pu, and $m_U = 1.34$ pu. As expected in both cases, the relay at Terminal S correctly calculated the location at about 0.9 pu and the relays at Terminals T and U calculated values considerably higher than 1 pu.

The faulted line section identification is based on exchanging the locally calculated values of m and comparing them with 1 pu. The line section that reports $m < (1 + \text{margin})$ pu is declared faulted, and the corresponding value of m is reported. The value of the margin is in the order of a few hundredths of per unit and accounts for small fault locating errors, as discussed in Section III, Subsection C.

In the previous examples, all three relays would indicate Section SP as the faulted section and report the fault location as 0.90 pu from Terminal S.

The following points are worth observing with respect to our faulted line section identification method:

- The values of m are communicated over the 87L channel using our patent-pending method without disturbing the 87L elements.
- For faults very close to the tap point, the three m values may be very similar, with more than one satisfying the $m < (1 + \text{margin})$ condition. This is acceptable, because all the m values would be close to 1 pu, indicating even more that the fault is near the tap point.
- If a given relay cannot use the enhanced algorithm shown in (15) and falls back to the single-ended method shown in (13), the overall scheme still works in principle (see more discussion in the following subsection). The only differences are the method (double-ended versus single-ended) and resulting accuracy of the m value calculation.

B. Fault Locating in Master-Slave Mode (Fallback Mode)

A three-terminal 87L scheme can operate in one of the following two modes:

- Master mode. All relays have access to all the currents of the protection zone; therefore, each relay makes an independent trip decision (each relay in the scheme is a master relay).
- Master-slave mode. Only one relay has access to all the currents of the protection zone; therefore, only that relay is a master and the other two relays (slave relays) supply data to the master relay and execute trip decisions received from the master relay.

The mode of operation of each relay in the scheme is determined by the communications channels available between relays. Consider the three-terminal 87L scheme shown in Fig. 15.

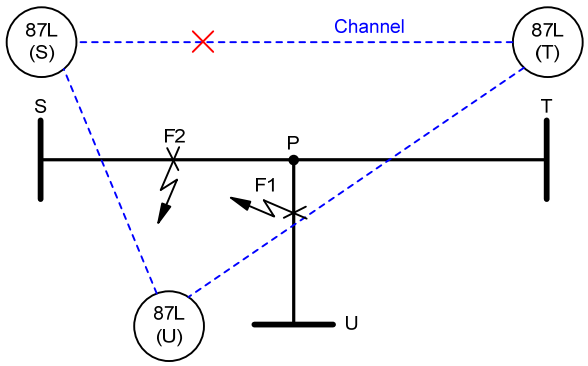

Fig. 15. A three-terminal 87L scheme operating in master-slave mode because communications are only available between Relays S and U and Relays U and T.

If the communications channel between Relays S and T becomes unavailable, then Relay S and Relay T do not have access to all the currents that make up the 87L protection zone and therefore cannot function independently. Relays S and T will switch from the master mode to the slave mode. Relay U has access to all of the currents and therefore will remain in the master mode. The master relay provides differential protection for the three-terminal line. For a fault within the protection zone, the master relay sends tripping commands to

the remote relays via in-band direct transfer trip bits. In addition to providing the line protection function, the master relay also provides the overall fault locating function for the scheme.

The master relay (Relay U) calculates the fault location as seen from its line terminal using (17c). The slave relays (Relays S and T) calculate the fault location using the single-ended method given by (13). The slave relays send their calculated *m* values to the master relay. Using its own calculated *m* value and those received from the slave relays, the master relay identifies the faulted line section by selecting the line terminal that calculated an *m* value less than 1. In our implementation, the master relay does not communicate the faulted section back to the slave relays. In this case, the true fault location has to be obtained from the master relay.

Consider Fault F1 on Section UP of the line in Fig. 15. For this case, Relay S calculates an *m* value greater than 1 ($m_S > 1$ pu); similarly, Relay T calculates an *m* value greater than 1 ($m_T > 1$ pu). Relays S and T use (13) to calculate their respective fault locations. Relay U (the master relay) calculates an *m* value less than 1 ($m_U < 1$) using (17c). Relays S and T transmit their calculated *m* values (m_S and m_T) to Relay U. Relay U determines the fault location by selecting the *m* value that is less than 1. For this example, the distance to the fault is m_U. This is the most accurate result, because m_U is calculated using the enhanced method shown in (17c).

Next, consider Fault F2 on Section SP. In this case, Relay S calculates $m_S < 1$ pu, Relay T calculates $m_T > 1$ pu, and Relay U calculates $m_U > 1$. As before, Relays S and T send their calculated *m* values to Relay U. Relay U then selects the faulted section as the one with an *m* value less than 1 and reports the distance to the fault as that value of *m*, in this case m_S. This value may have some inaccuracy, because m_S has been calculated in Relay S using the single-ended method shown in (13). In this particular case, Relay U could theoretically calculate the tap-point voltage and current and execute the method shown in (17c) for the remote line segment. However, the designers opted against this complication in the actual implementation of the fault locating algorithm. In summary, obtaining data from all relays in an 87L scheme enables the scheme to correctly identify the faulted line section and determine the fault location with relatively good accuracy, even when the scheme is operating in master-slave mode.

C. Simulation Results

We modeled a three-terminal 525 kV line in a Real Time Digital Simulator (RTDS®) to illustrate the performance of the three-terminal fault locating algorithm. The three-terminal line modeled in the RTDS is shown in Fig. 14. Sources S and U have the same strength, and Source T is the weakest source with an impedance three times that of Sources S and U. The line segments and sources are homogeneous, and the lengths of the line segments are as follows: Segment SP = 100 kilometers, Segment TP = 25 kilometers, and Segment UP = 50 kilometers. Due to the lengths of the line segments, charging current compensation was enabled at all line terminals. The line draws a charging current of approximately 250 A.

Table II shows the fault type, fault resistance, line segment in which the fault was simulated, actual distance to the fault from the line segment terminal, identified faulted line segment, distance calculated from the local line terminal using the double-ended fault locating method, and percentage error.

From Table II, we can see that for each case, the double-ended fault locating algorithm selected the correct faulted line segment. Table II shows a maximum error of 0.75 percent for a fault resistance of 10 ohms and an error of 6.05 percent for a fault resistance of 100 ohms.

Factors that affect the accuracy of the fault location are discussed in the following subsection.

D. Factors That Affect Accuracy

The three-ended fault locating algorithm is the same as for a two-terminal line; therefore, the factors that affect the accuracy of the algorithm are the same as those discussed in Section III, Subsection C.

For this discussion, we concentrate on two factors, namely the fault resistance and the asymmetry (lack of transposition) of the transmission line. The errors for all of the faults in Table II are directly related to the magnitude of the fault resistance and the asymmetry of the transmission line. The method used to calculate the distance to the fault is impedance-based, using the differential current for polarizing. Even though we state that the line is transposed, the fault current contributions from the line terminals are not perfectly in phase with one another due to the asymmetry of the line as seen from the fault point. This nonhomogeneity of the system, when viewed from the location of the fault, results in the total

TABLE II
PERFORMANCE OF THE DOUBLE-ENDED FAULT LOCATING ALGORITHM FOR FAULTS ON A THREE-TERMINAL LINE

Fault Type	Fault Resistance (ohms)	Simulated Line Segment	Actual Distance (km)	Identified Line Segment	Calculated Distance (km)	Error (%)
AG	10	SP	75	SP	74.28	0.41
BC	10	TP	18.75	TP	19.7	0.54
CAG	10	UP	12.5	UP	11.18	0.75
ABC	10	SP	25	SP	24.74	0.15
ABG	100	SP	25	SP	14.41	6.05

fault current not being in phase with the fault current contributed by each of the line terminals. The fault resistance magnifies this source of error.

In our case, the fault currents contributed by the strongest terminals (S and U) lead the total fault current, and the fault current contributed by Terminal T lags the total fault current. The result of this is that for faults on line segments connected to the strongest sources, the fault locating algorithm overreaches (i.e., calculates a fault location closer to the terminal than the actual fault location) because the strong terminal currents lead the fault current. The 100-ohm fault illustrates how the fault resistance magnifies this phenomenon.

For faults located on line segments connected to the weakest terminal, the fault locating algorithm underreaches (i.e., locates the fault farther away from the line terminal than the actual fault location) because the weak terminal current lags the fault current.

V. Four-Ended Fault Locating in 87L Relays

A. Faulted Section Identification and Fault Location Determination

Consider the four-terminal line shown in Fig. 16.

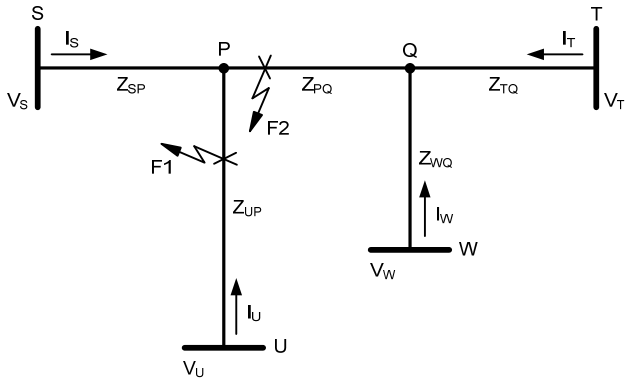

Fig. 16. Four-terminal line.

In a four-terminal line application, the fault locating algorithm is executed in two or three steps, depending on the actual fault location.

First, each relay assumes the fault is in its local section. If the assumption is true for one relay, this relay will calculate a value of *m* less than 1 pu, and the fault locating process will continue, as explained in the previous section for the three-terminal line. For example, for Fault F1 in Fig. 16, Relay U will calculate $m < 1$ pu, and all four relays will report Section UP as faulted.

If no relays calculate $m < 1$ pu, the fault must be in the middle section (PQ) between the two taps (Fault F2 in Fig. 16). If so, the voltages and currents at both tap points (P and Q) must be calculated next. Knowing that the local line sections are free from faults, each relay calculates the equivalent currents and voltages for the PQ section of the line using the voltage drop equation for the unfaulted section.

The relay at Terminal S calculates:

$$I_P = I_S + I_U \text{ and } V_P = V_S - Z_{SP} \bullet I_S \quad (18a)$$

The relay at Terminal U calculates:

$$I_P = I_U + I_S \text{ and } V_P = V_U - Z_{UP} \bullet I_U \quad (18b)$$

The relay at Terminal T calculates:

$$I_Q = I_T + I_W \text{ and } V_Q = V_T - Z_{TQ} \bullet I_T \quad (18c)$$

The relay at Terminal W calculates:

$$I_Q = I_W + I_T \text{ and } V_Q = V_W - Z_{WQ} \bullet I_W \quad (18d)$$

In order to calculate the currents in these equations, each relay is provided with a setting indicating the specific remote relay that is installed on the line section connected to the same tap (Relays S and U monitor line sections that connect to Tap Point P, and Relays T and W monitor line sections that connect to Tap Point Q).

Having the P (or Q) currents and voltages calculated and having the Z_{PQ} impedance as a setting, each relay executes (15) and obtains a coherent fault locating result. Relays S and U report *m* pu as the distance to the fault from Tap Point P, and Relays T and W report (1 – m) pu as the distance to the fault from Tap Point Q.

B. Fault Locating in Fallback Mode

In our four-terminal 87L implementation, data are exchanged between relays using Ethernet as the communications medium. Because of the use of Ethernet, all relays are either in the master mode or the 87L scheme is not operational [5].

In the master mode, all relays have access to all the remote currents and the distance to the fault is computed as explained in the previous subsection.

When the 87L scheme is not operational, the fault locating algorithm switches from the multiterminal mode to single-terminal mode. As a result, the fault locating accuracy is typically degraded.

However, the scheme will still be able to correctly determine the faulted line section. A fault between any line terminal and a tap point will result in one relay calculating an *m* value less than 1 and all other relays calculating *m* values greater than 1. For a fault between the two tap points, all relays will calculate *m* values greater than 1. Because there is no communication between the individual relays, it is not possible to perform fault locating in real time. Fault locating has to be done offline, either by manually retrieving and processing data from the relays or by using an offline program that retrieves and processes the data.

The following subsection discusses the fault locating accuracy for the four-terminal operating mode and the factors that influence this accuracy.

C. Factors That Affect Fault Locating Accuracy

The four-ended fault locating algorithm is an extension of the two-ended algorithm. Therefore, the accuracy of the four-ended algorithm is affected by the factors described in Section III, Subsection C, except for an important difference: the effect of the time-alignment method. In the two-ended mode, current alignment can be done by using either the ping-pong method (channel-based alignment) or by using a

common time reference. In the four-ended mode, Ethernet is used to exchange data between relays and the ping-pong method cannot be used because channel symmetry cannot be guaranteed. Therefore, an external time reference is used for current alignment.

There are two ways of providing the external time reference:

- Using local IRIG-B signals (derived from local GPS clocks or from a network-based terrestrial time-distribution system, such as over a synchronous optical network [SONET]).
- Using the Precision Time Protocol (PTP) IEEE C37.238.

When the time reference is provided by local IRIG-B signals, each relay must monitor the integrity of its clock signal. If a clock loses its GPS lock, its time quality will degrade and the timing accuracy of the data from that relay cannot be guaranteed. The scheme currents cannot be aligned with enough accuracy to facilitate multi-ended fault locating, and the fault locator needs to fall back to the single-ended method.

When the fault locator falls back to the single-ended method, the accuracy will degrade for the reasons discussed in Section III, Subsection C. However, if the fault is located between a line terminal and a tap point, the fault locating accuracy for the relay located at the terminal of the faulted line section is primarily influenced by the fault resistance (assuming that the line positive- and zero-sequence impedance values are fairly accurate). When the fault resistance is relatively small, the accuracy of the single-ended method for faults between the line terminal and the tap point for the relay connected to that line terminal will be fairly accurate; fault location estimation for all other relays will be significantly off because of the infeed effect. The higher the fault resistance, the more important role the currents from the remote terminals will play and the larger the error will be. Therefore, the relay that calculates an *m* value less than 1 will have the most accurate distance-to-fault value in the scheme.

For faults between the two tap points, the accuracy of the single-ended fault locating algorithm will be determined by the fault resistance, the distance to the fault from the tap point, the system nonhomogeneity, and the strength of the sources at the line terminals. As mentioned in Section V, Subsection A, all relays will calculate an *m* value greater than 1 for a fault between the two tap points. However, if the fault is located closer to one tap point than the other, in general, the relays that are adjacent to that tap point will yield a better result than those relays adjacent to the tap point farthest from the fault. In this case, the strength of the source behind each relay plays a significant role.

When IEEE C37.238 provides the time reference, all relays are synchronized via Ethernet. This means that no relay clock loses synchronism with respect to the other relays while communication between the relays exists. Therefore, no time-alignment error exists in this mode as long as the source of the IEEE C37.238 timing signal is accurate.

VI. Conclusion

Embedding multi-ended fault locating in 87L relays brings many advantages. A single system serves both protection and multi-ended fault locating functions, allowing savings in communications, time synchronization, material costs, and engineering.

This paper presents a novel multi-ended fault locating method designed specifically for ease of integration in 87L schemes. The method, which uses the differential current, improves the numerical accuracy of fault locating compared with single-ended methods and indicates the faulted line section in three- and four-terminal applications. Practical implementation aspects are considered to address cases of loss of communications or degraded precision of data alignment.

VII. References

[1] H. J. Altuve Ferrer and E. O. Schweitzer, III (eds.), *Modern Solutions for Protection, Control, and Monitoring of Electric Power Systems*. Schweitzer Engineering Laboratories, Inc., Pullman, WA, 2010.

[2] E. O. Schweitzer, III, A. Guzmán, M. V. Mynam, V. Skendzic, B. Kasztenny, and S. Marx, "Locating Faults by the Traveling Waves They Launch," proceedings of the 40th Annual Western Protective Relay Conference, Spokane, WA, October 2013.

[3] E. O. Schweitzer, III, "Evaluation and Development of Transmission Line Fault-Locating Techniques Which Use Sinusoidal Steady-State Information," proceedings of the 9th Annual Western Protective Relay Conference, Spokane, WA, October 1982.

[4] E. O. Schweitzer, III, "A Review of Impedance-Based Fault Locating Experience," proceedings of 15th Annual Western Protective Relay Conference, Spokane, WA, October 1988.

[5] D. A. Tziouvaras, J. Roberts, and G. Benmouyal, "New Multi-Ended Fault Location Design for Two- or Three-Terminal Lines," proceedings of the 7th International Conference on Developments in Power System Protection, Amsterdam, Netherlands, April 2001.

[6] Y. Gong, M. Mynam, A. Guzmán, G. Benmouyal, and B. Shulim, "Automated Fault Location System for Nonhomogeneous Transmission Networks," proceedings of the 65th Annual Conference for Protective Relay Engineers, College Station, TX, April 2012.

[7] K. Zimmerman and D. Costello, "Impedance-Based Fault Location Experience," proceedings of the 58th Annual Conference for Protective Relay Engineers, College Station, TX, April 2005.

[8] B. Kasztenny, G. Benmouyal, H. J. Altuve, and N. Fischer, "Tutorial on Operating Characteristics of Microprocessor-Based Multiterminal Line Current Differential Relays," proceedings of the 38th Annual Western Protective Relay Conference, Spokane, WA, October 2011.

[9] IEEE Standard C37.114-2004, IEEE Guide for Determining Fault Location on AC Transmission and Distribution Lines.

VIII. BIOGRAPHIES

Omar Avendano received his BS in electrical engineering from Simón Bolívar University in Caracas, Venezuela, in 1984. He worked for 12 years in the manufacturing and design of uninterruptible power supply systems applied to critical industrial loads. During this time, he designed and developed automated controls for ac and dc distribution centers and performed protective relay coordination studies. He joined PacifiCorp in November 2001, where he served as the lead senior protection and control engineer for 10 years, developing protection designs for transmission and distribution. In 2012, he joined Portland General Electric in the role of Senior Protection Engineer and has continued to develop extra-high-voltage transmission and generation protection.

Bogdan Kasztenny is the research and development director of technology at Schweitzer Engineering Laboratories, Inc. He has over 23 years of expertise in power system protection and control, including ten years of academic career and ten years of industrial experience, developing, promoting, and supporting many protection and control products. Dr. Kasztenny is an IEEE Fellow, Senior Fulbright Fellow, Canadian representative of CIGRE Study Committee B5, registered professional engineer in the province of Ontario, and an adjunct professor at the University of Western Ontario. Since 2011, Dr. Kasztenny has served on the Western Protective Relay Conference Program Committee. He has authored about 200 technical papers and holds 20 patents.

Héctor J. Altuve received his BSEE degree in 1969 from the Central University of Las Villas in Santa Clara, Cuba, and his Ph.D. in 1981 from Kiev Polytechnic Institute in Kiev, Ukraine. From 1969 until 1993, Dr. Altuve served on the faculty of the Electrical Engineering School at the Central University of Las Villas. From 1993 to 2000, he served as professor of the Graduate Doctoral Program in the Mechanical and Electrical Engineering School at the Autonomous University of Nuevo León in Monterrey, Mexico. In 1999 through 2000, he was the Schweitzer Visiting Professor in the Department of Electrical Engineering at Washington State University. Dr. Altuve joined Schweitzer Engineering Laboratories, Inc. (SEL) in January 2001, where he is currently a distinguished engineer and dean of SEL University. He has authored and coauthored more than 100 technical papers and several books and holds four patents. His main research interests are in power system protection, control, and monitoring. Dr. Altuve is an IEEE senior member.

Bin Le received his BSEE from Shanghai Jiao Tong University in 2005 and an MSEE from the University of Texas at Austin in 2008. He has been employed by Schweitzer Engineering Laboratories, Inc. since 2008. Mr. Le currently holds the position of lead power engineer in the research and development division. He is a member of IEEE and a professional engineer registered in the state of Washington.

Normann Fischer received a Higher Diploma in Technology, with honors, from Technikon Witwatersrand, Johannesburg, South Africa, in 1988; a BSEE, with honors, from the University of Cape Town in 1993; and an MSEE from the University of Idaho in 2005. He joined Eskom as a protection technician in 1984 and was a senior design engineer in the Eskom protection design department for three years. He then joined IST Energy as a senior design engineer in 1996. In 1999, Mr. Fischer joined Schweitzer Engineering Laboratories, Inc., where he is currently a fellow engineer in the research and development division. He was a registered professional engineer in South Africa and a member of the South African Institute of Electrical Engineers. He is currently a senior member of IEEE and a member of ASEE.